Table of Content

1. **Materials.** S2
2. **Preparation of DNA Constructs for Mechanical Unfolding through Different Residues.** S2
3. **Single-Molecule Mechanical Unfolding Experiments.** S3
4. **Calculation of Phosphorus-to-Phosphorus Distance in G-quadruplex.** S4
5. **Sequences of G-quadruplex Forming DNA.** S5
6. **Synthesis and Click Chemistry Linkage of Modified dsDNA.** S6
7. **Force-Extension (F-X) Curves.** S7
8. **Change-in-contour-length.** S8
9. **Structural Fingerprinting at the Single Molecular Level.** S9
10. **Circular Dichroism Spectra.** S11
11. **Overlapping of PDB Structures.** S12
12. **Proposed Energy Diagrams.** S13
13. **G-quadruplex Stalling Transcription.** S14
14. **SPR Experiments.** S15
15. **Supporting Reference.** S17

1. Materials.

Oligonucleotides purchased from Integrated DNA Technology (IDT) were purified by PAGE gel. Restriction enzymes were obtained from New England Biolabs (NEB). Streptavidin or anti-digoxigenin antibody coated polystyrene beads were purchased from Spherotech (Lake Forest, IL). Chemicals with > 99% purity were purchased from VWR. The 5'-*O*-dimethoxytrityl-N^2-*tert*-butylphenoxyacetyl-2'-deoxyriboguanosine 3'-*O*-ethynylphosphinoamidite was synthesized as reported. [S1] Telomestatin derivatives were synthesized and characterized as described in previous reports. [S2,S3]

2. Preparation of DNA Constructs for Mechanical Unfolding through Different Residues.

DNA constructs were synthesized according to reported procedures (Figure S1). [S4] Briefly, telomeric DNA , 5′-TTA$(GGGTTA)_4$, was synthesized in an ABI DNA synthesizer (Applied Biosystem, Foster City, CA) using $O^{5'}$-dimethoxytrityl-2'-deoxyribonucleoside-$O^{3'}$-phosphoramidites and alkyne-modified phosphinoamidite (5'-*O*-dimethoxytrityl-N^2-*tert*-butylphenoxyacetyl-2'-deoxyriboguanosine 3'-*O*-ethynylphosphinoamidite, see Materials). The crude oligonucleotides were purified by RP-HPLC. DNA concentrations were evaluated by Nano-drop ND-1000 (Nano-drop Technologies, Wilmington, DE).

These ethynyl-modified single-stranded DNA sequences were tethered between the two 2028 bp dsDNA handles, which were prepared by PCR using the pBR322 plasmid (site 629-2961^{th}) as the template. The azide and the biotin groups in one handle were separately introduced at the 5′ ends by using primers with respective modifications. In another 2028 bp handle, azide and digoxigenin were similarly introduced. These two 2028-bp dsDNA handles were mixed with the alkyne modified single-stranded DNA sequences by the copper-catalyzed azide-alkyne cycloaddition (CuAAC) as described in the previous paper [S4,S5] The CuBr in the click chemistry reaction was removed by addition of equal amount of EDTA, which was followed by ethanol precipitation. This preparation produced ssDNA sequence attached to the two dsDNA handles through the residues in the G-tetrad planes. These constructs were named as Top, Middle, and Bottom to reflect the attachment of the two 2028 bp handles through the G residues in the top, middle, and bottom G-tretrads, respectively. Similarly, reported

procedure was used to prepare the constructs, [5′-L2], [5′-L3], [L1-3′], [L2-3′], and [L1-L3], that had the loop residues connected to the 2028 bp DNA handles. [S1,S4]

3. Single-Molecule Mechanical Unfolding Experiments.

Mechanical unfolding on the DNA constructs prepared above was carried out in dual–trap optical tweezers [S6] in a 10 mM Tris buffer (pH 7.4) supplemented with 100 mM KCl with or without 100 nM telomestatin derivative L2H2-6OTD (K_d=10.8 nM) at 23 ºC. [S1] Before the mechanical unfolding experiments, individual DNA constructs were tethered to the two optically trapped polystyrene beads that were coated with streptavidin and digoxigenin antibody respectively. One of the beads was moved away from another by a steerable mirror, leading to increased tension in the DNA tether. The resultant force-extension (*F-X*) curves were recorded in the range of 0-65 pN at 1000 Hz with a loading rate of 5.5 pN/s by the Labview program (National Instruments, Austin, TX). The observation of the 65 pN plateau in the *F-X* curves indicated the DNA tether was single molecule in nature. [S7]

These *F-X* curves were treated in a Matlab program (The MathWorks, Natick, MA) by a Savitzky-Golay filter with a bandwidth of 10 ms. At each unfolding event, the change in extension (Δx) was measured from the difference between stretching and relaxing curves at the unfolding force. The change in contour length (ΔL) was then calculated with a modified worm-like-chain model (WLC, see eqn (S1)). [S8]

$$\frac{\Delta x}{\Delta L} = 1 - \frac{1}{2}\sqrt{\frac{k_B T}{FP}} + FS \quad \text{.....eqn (S1)}$$

Where, L is the contour length, k_B is the Boltzmann constant, T is absolute temperature, P is the persistence length (50.8 nm), [S9] and S is the stretching modulus (1243 pN). [S9] Standard deviations were obtained from triplicate experiments wherever appropriate.

Equation proposed by Dudko (eqn (2)) [S10] was used to fit the unfolding force histogram,

$$p(F) \propto \frac{K(F)}{r} \exp\left\{\frac{k_{unfold}}{x^{\dagger}r} - \frac{k(F)}{x^{\dagger}r}\left(1 - \frac{x^{\dagger}F}{\Delta G^{\dagger}}\nu\right)^{\left(1-\frac{1}{\nu}\right)}\right\} \text{.....eqn (S2)}$$

where $k(F) = k_{unfold}\left(1 - \frac{x^{\dagger}F}{\Delta G^{\dagger}}\nu\right)^{\frac{1}{\nu}-1} exp\left\{\Delta G^{\neq}\left[1 - \left(1 - \frac{x^{\dagger}F}{\Delta G^{\dagger}}\nu\right)^{\frac{1}{\nu}}\right]\right\}$

and k(F) and k_{unfold} are the unfolding rate constants at the force F and 0 pN, respectively, $x^{\dagger}$ is the transition state distance from the folded state, $\Delta G^{\dagger}$ is the height of the energy barrier and ν describes the shape of the energy barrier (ν=1/2 for a sharp, cusp-like barrier).

4. Calculation of Phosphorus-to-Phosphorus Distance in G-quadruplex.

To calculate the distance between two different phosphorus atoms (see pa and pb in eqn(S3)), we retrieved the 3D coordinate data (x, y, and z) from the RCSB Protein Data Bank (PDB). We then calculated the distance between two phosphorus atoms using the function:

$$\mathrm{D} = \sqrt{\left(x_{\mathrm{pa}} - x_{\mathrm{pb}}\right)^2 + \left(\mathrm{y_{pa}} - \mathrm{y_{pb}}\right)^2 + \left(\mathrm{z_{pa}} - \mathrm{z_{pb}}\right)^2} \text{ ..... eqn (S3)}$$

The distance calculated this way was identical to that directly measured from the 3D structure in PDB. Differences of the distance for the same pair of the phosphorus-phosphorus atoms with and without the telomestatin analogue were grouped into specific regions (G-tetrads (GQ), Loop 1 (L1), Loop 2 (L2), and Loop 3 (L3)), and plotted as histograms (Figure 4).

5. Sequences of G-quadruplex Forming DNA.

Table S1. *G-quadruplex sequences with modifications shown in bold for mechanical unfolding through different geometries. In the Top, Middle, and Bottom geometries, the phosphate backbone in the 3′ of specific nucleotide is modified with alkyne group. In the L2-3', 5'- L2, 5'-L3 constructs, the residues are modified with azide.* [S1,S5] *In the L1-L3 geometry, the modification involves 5-octadiynyl-deoxyuridine.* [S1,S5]

Geometry	**Sequence**
Top	5'-TTA **G**GG TTA GGG TTA GGG TTA **G**GG TTA-3'
Middle	5'-TTA G**G**G TTA GGG TTA GGG TTA G**G**G TTA-3'
Bottom	5'-TTA GG**G** TTA GGG TTA GGG TTA GG**G** TTA-3'
L2-3'	5'-TTA GGG TTA GGG T**T**A GGG TTA GGG TTA GCC AGC AAG ACG TAG CCC AGC GCG TC-3'
5'-L2	5'-GGC CGA CGC GCT GGG CTA CGT CTT GCT GGC TTA GGG TTA GGG T**T**A GGG TTA GGG TTA -3'
L1-3'	5'-TTA GGG T**T**A GGG TTA GGG TTA GGG TTA GCC AGC AAG ACG TAG CCC AGC GCG TC-3'
5'-L3	5'-GGC CGA CGC GCT GGG CTA CGT CTT GCT GGC TTA GGG TTA GGG TTA GGG T**T**A GGG TTA-3'
L1-L3	5'-TTA GGG T**T**A GGG TTA GGG T**T**A GGG TTA -3'

6. Synthesis and Click Chemistry Linkage of Modified dsDNA.

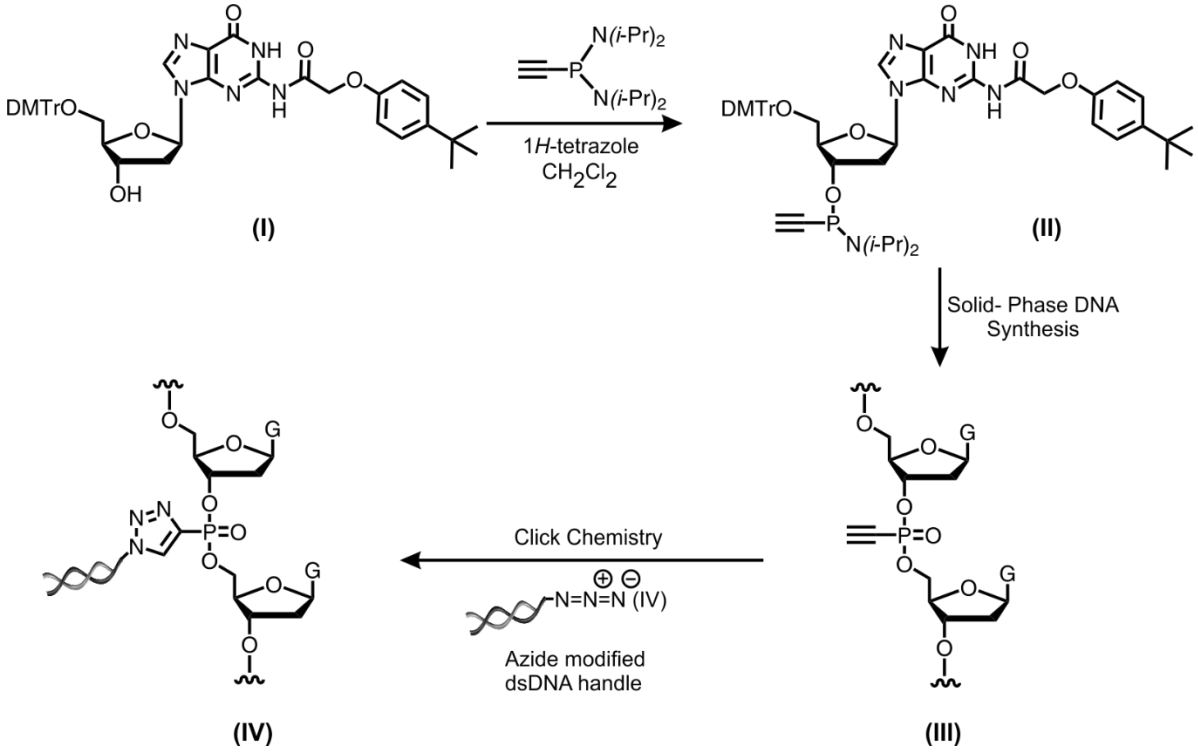

Figure S1. *An alkyne-modified guanine residue (II) was prepared from compound I. Solid-phase synthesis of oligodeoxynucleotides (III) was performed from (II). Click chemistry was used to link alkyne group of (III) to the azide modified dsDNA handle.*

7. Force-Extension (F-X) Curves.

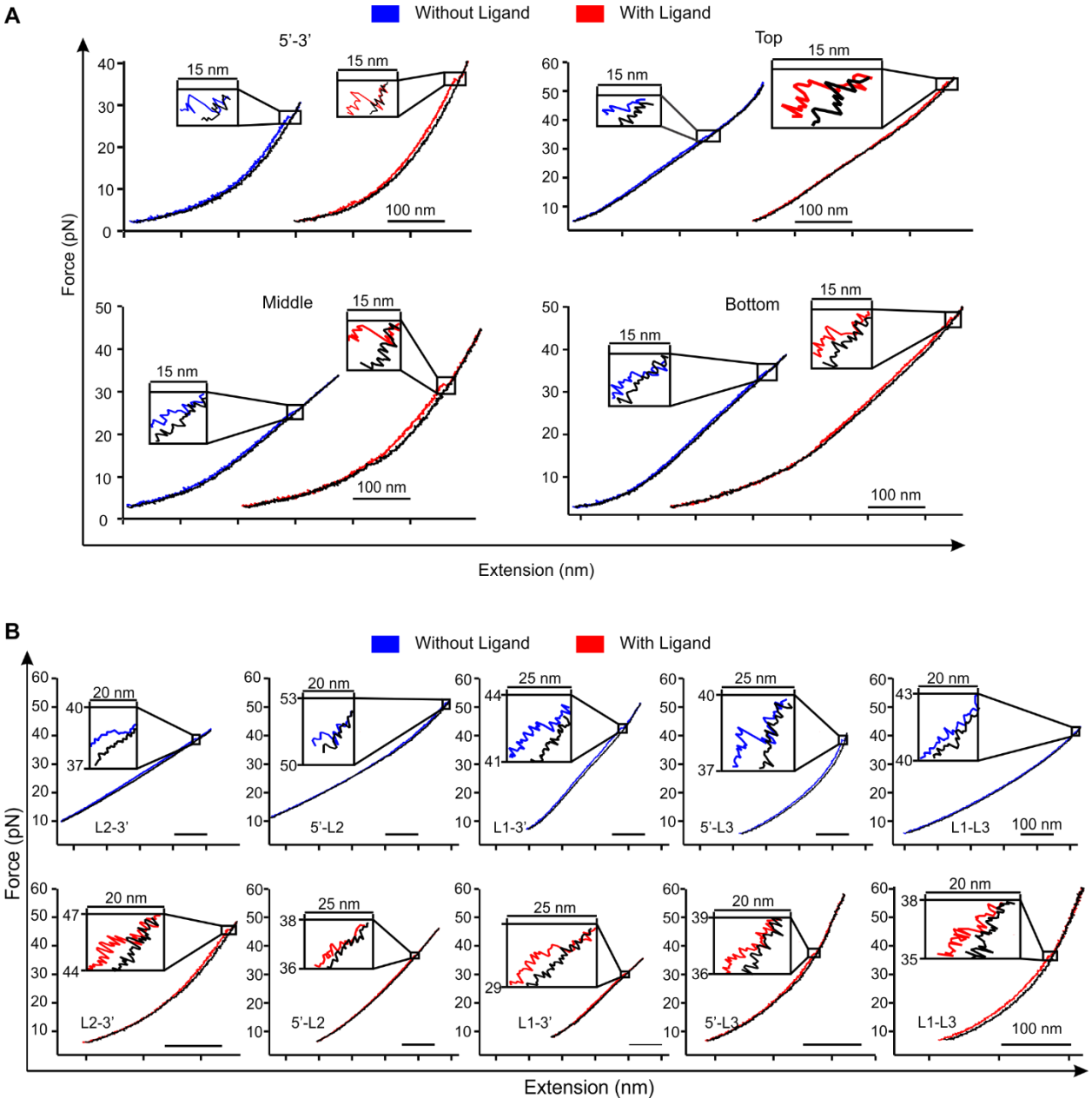

Figure S2. *F-X curves of the unfolding through (A) G-tetrads and (B) loops. Blue and red curves represent stretching traces without and with the L2H2-6OTD ligand respectively. Black curves represent the relaxing traces.*

8. Change-in-contour-length.

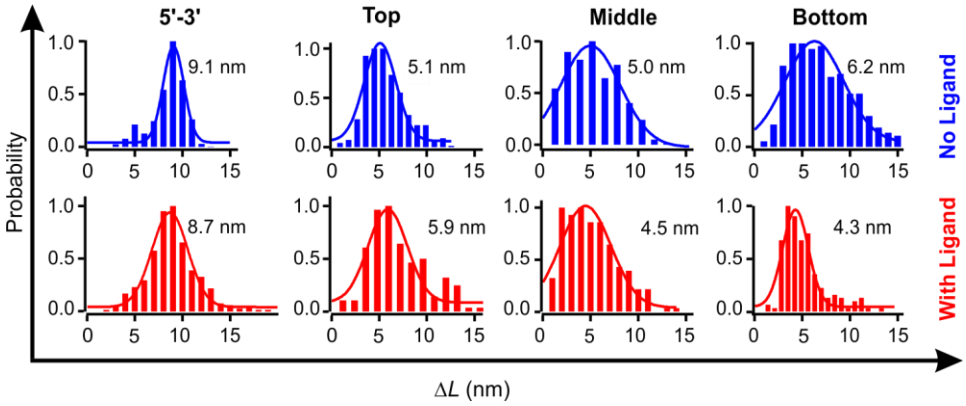

Figure S3. *Change-in-contour-length (ΔL) histograms for the G-quadruplexes unfolded from different G-tetrad planes without (blue) and with 100 nM L2H2-6OTD ligand (red) in 10 mM Tris (pH 7.4) supplemented with 100 mM KCl.*

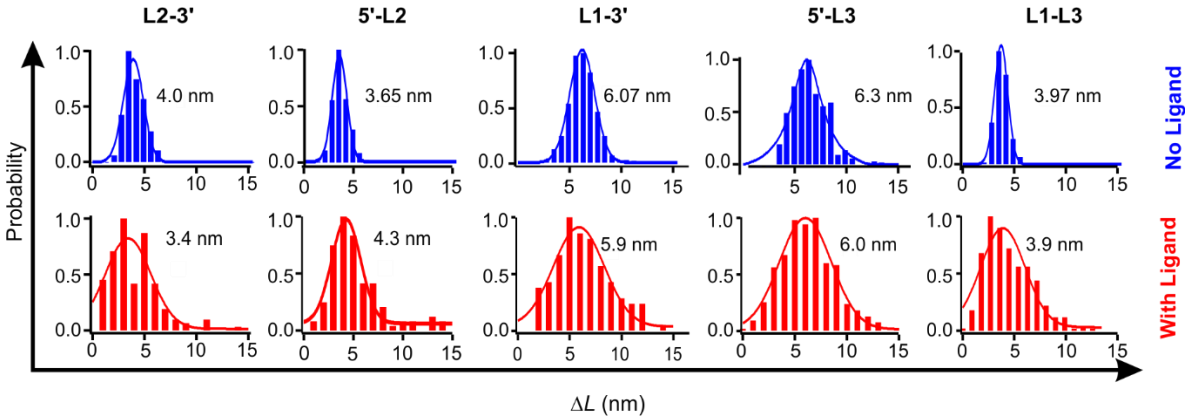

Figure S4. *Change-in-contour-length (ΔL) histograms for the G-quadruplexes unfolded from different loop-involving geometries without (blue) and with 100 nM L2H2-6OTD ligand (red) in 10 mM Tris (pH 7.4) supplemented with 100 mM KCl.*

9. Structural Fingerprinting at the Single Molecular Level.

The conformation of the G-quadruplex was determined by the root mean square deviation analysis of the end-to-end distance (x) obtained from the mechanical unfolding experiments (eqn S4) and that measured by NMR or X-ray crystallography.

$x = n \times L_{sn} - \Delta L$ …….. eqn (S4)

where x is the residue-to-residue distance between the two handling residues, n is the number of nucleotides, L_{sn} is the contour length for single nucleotide, and ΔL is the change in contour length upon unfolding of a structure.

From specific NMR or X-ray crystallography structures [S11,S12,S13,S14,S15,S16], the end-to-end distances ($x_{measurement}$) between the two phosphorus atoms that respectively correspond to the two unfolding residues were measured. Each $x_{measurement}$ was evaluated against the corresponding residue-to-residue distance obtained by mechanical unfolding (x) as square difference $(x_{measurement}-x)^2$. A total of 9 square differences, which correspond to the unfolding geometries from the Top, Middle, Bottom, 5′-3′, L2-3′, 5′-L2, L1-3′, 5′-L3, and L1-L3, respectively, were calculated as root mean square deviation (RMSD). The smaller the RMSD, the better the structural matching between experimentally determined conformation and that from NMR or X-ray methods. [S5] The RMSD analysis shows that hybrid-1 is the best matching conformation (Figure S5).

It is noteworthy that the conformation (hybrid-1) obtained by our single-molecule fingerprinting method is different from literature. [S12,S17] The buffer condition for our experiment was 10 mM Tris supplemented with 100 mM KCl (pH 7.4), while in one of the high-resolution studies, the buffer condition used was 25 mM HEPES, 110 mM KCl, 130 mM $CaCl_2$, 1mM $MgCl_2$, and 10% D_2O (pH 7.5). [S17] These two buffer conditions are so different that conformation obtained from the high-resolution experiment cannot be applied here. In addition, the sequences used were different (in the reference S17, $TTA(GGG)_4TT$ was used, whereas we used $TTA(GGG)_4TTA$ here). In the other paper [S12], the sequence used was the same as ours. However, the buffer they used, 25 mM K-phosphate buffer (pH 7.0) and 70 mM KCl, was different from ours. [S12] Even under these conditions, the authors found 65% conformation was hybrid-2 while hybrid-1 was also observed. It is noteworthy that in these NMR studies, DNA in mM or sub-mM ranges was used whereas in our single-molecule method, the effective concentration was in the nM range. [S9] This significant difference in DNA concentration may also cause difference in conformations.

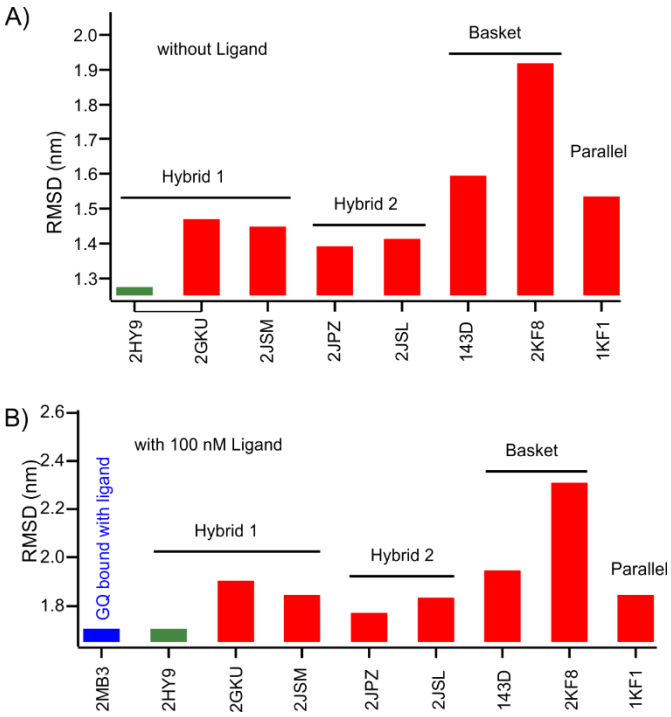

Figure S5. Root Mean Square Differences (RMSD) of the inter-residue distances (from the Top, Middle, Bottom, 5'-3', L2-3', 5'-L2, L1-3', 5'-L3, and L1-L3 unfolding geometries) between known PDB structures and mechanical unfolding measurements without (A) and with (B) ligand. Notice data in (A) were slightly different from previous reported values [S1] since we remeasured all ΔL values using the ΔL versus Force plots. [S5] In (B), we found the two best matching structures (2MB3 and 2HY9) both assume the hybrid-1 conformation. Since the 2MB3 represents the conformation of the G-quadruplex bound with the same ligand L2H2-6OTD as used here, this result validates the accuracy of our RMSD analyses.

10. Circular Dichroism Spectra.

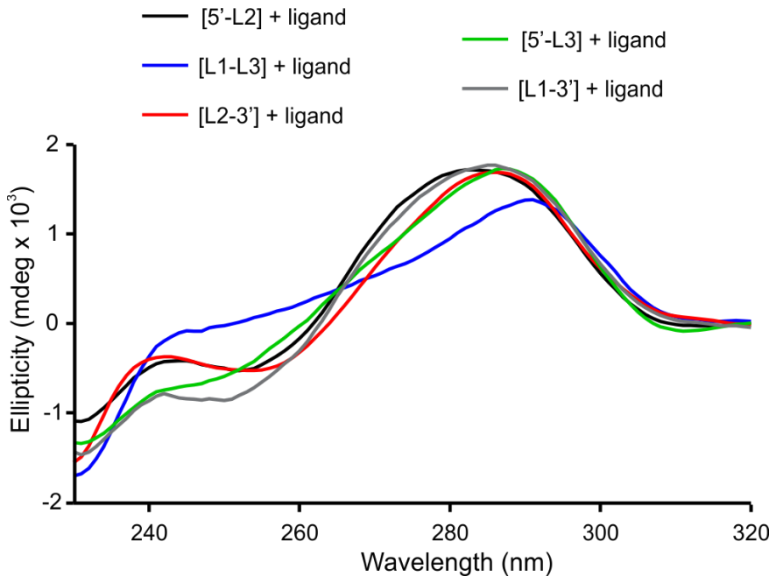

Figure S6. *Circular Dichroism spectra of the G-quadruplex constructs (5 µM) that are modified with click chemistry groups in different loops with 5 µM L2H2-6OTD ligand in a buffer containing 10 mM Tris (pH 7.4) and 100 mM KCl. See Table S1 for the corresponding sequences. CD spectra for DNA constructs without ligand and DNA constructs modified at the G-tetrad planes were reported in reference* [S1,S5].

11.Overlapping of PDB Structures.

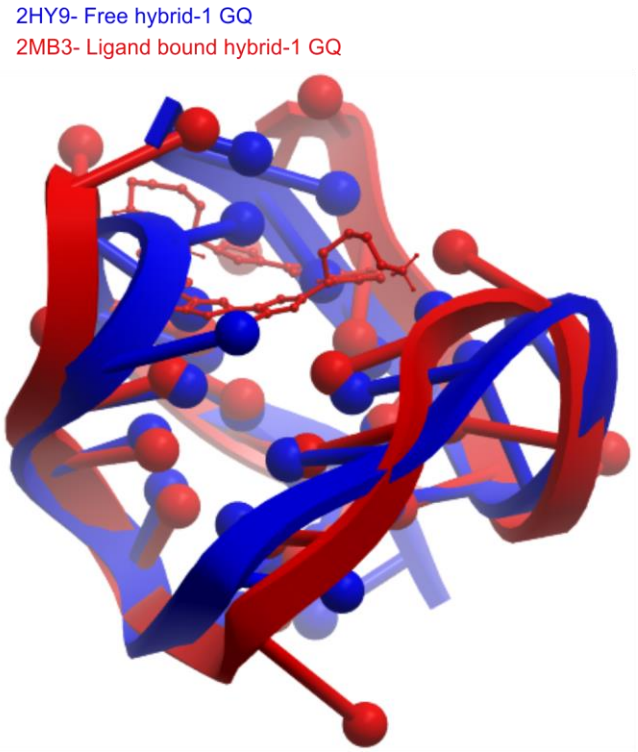

Figure S7. *Overlapping of free (blue) and ligand-bound (red) G-quadruplexes showing conformational difference between the two structures.*

12.Proposed Energy Diagrams.

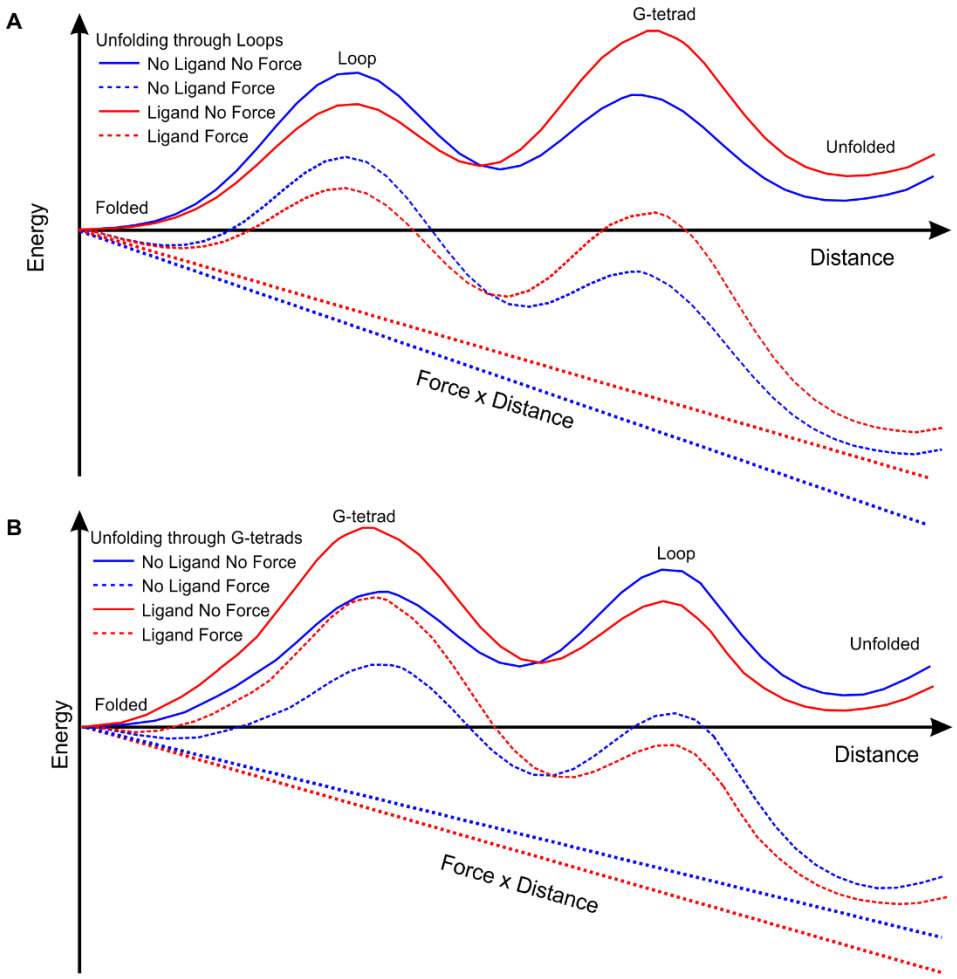

Figure S8. *Schematic of energy diagrams for unfolding of G-quadruplexes through the loops (A) and the G-tetrads (B). For clarity, the free energies of folded conformations with and without ligands have been offset to have the same values. Note the slopes of straight Force × Distance lines represent the force magnitudes. After application of force, the energy diagrams (solid curves) without force become those with force (dotted curves). In addition, for clarity, the energy barriers corresponding to the unfoldings of different G-tetrads* [S1] *are combined into a single energy barrier designated as G-tetrad.*

13.G-quadruplex Stalling Transcription.

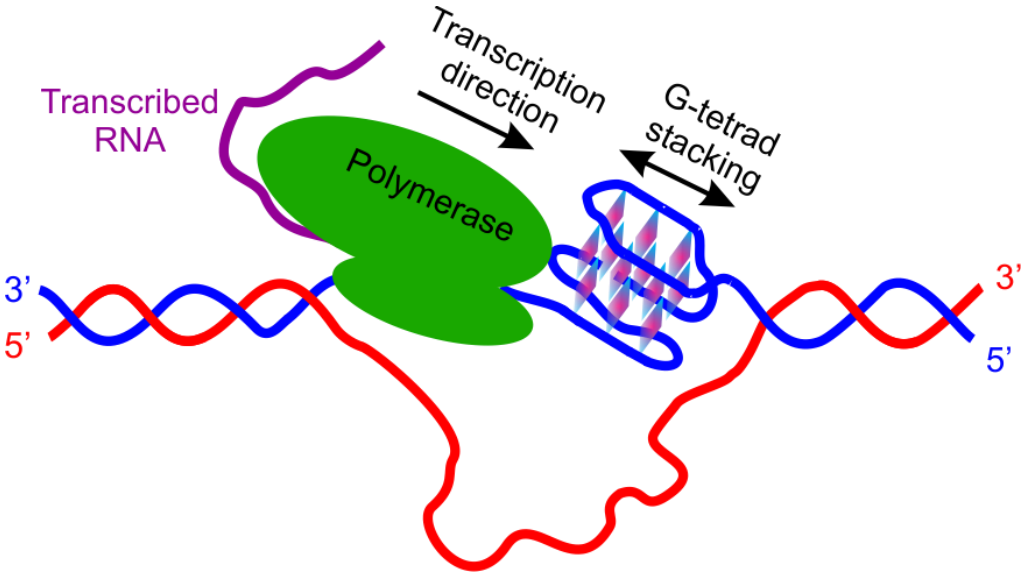

Figure S9. *Schematic of a RNA polymerase (green) stalled by a G-quadruplex in the template DNA strand (blue). The complementary DNA strand is shown in red. Notice the direction of the RNA transcription applies a force along the G-tetrad stacking direction in the G-quadruplex.*

14. SPR Experiments.

Surface plasmon resonance (SPR) measurements were performed with a four-channel BIAcore T200 instrument (GE Healthcare) and streptavidin-coated sensor chip (Biacore SA-chip). All measurements were performed at 25 ºC using a running buffer (HEPES buffer), which was prepared using 10 mM HEPES (pH 7.4), 150 mM NaCl, 3 mM EDTA and 0.005% surfactant P20. We have used two biotinylated DNA; telo22 (5'-biotin-d[AGG GTT AGG GTT AGG GTT AGG G]-3') and telo22-iAz (5'-biotin-d[AGG GTT AGG GTT AGG GT/AzideT/ AGG G]-3'), which were purchased from IDT (Integrated DNA Technologies). All DNAs were denatured in HEPES buffer at 99 ºC for 5 min, then allowed to cool down to room temperature overnight. The flow cells 2 and 4 were used to immobilize the DNA, while the 1 and 3 flow cells were left blank as a control. After conditioning the surface with three 1-min injections of 1 M NaCl/50 mM NaOH, a solution of DNA samples (100 nM in running buffer) was injected at a rate of 10 μL/min. For binding experiments, a stock solution of L2H2-6OTD was prepared at 10 μM concentration in running buffer, and desired experimental concentration was prepared by serial dilutions from stock solution. The experimental solutions at concentrations from 2 to 1000 nM were injected through the DNA and blank flow cells at a rate of 30 μL/min. To remove any remaining bound compound after the dissociation phase of the sensorgram, a low pH glycine regeneration buffer was used (10 mM glycine at pH 2.0). The baseline was then reestablished, and the next sample with different compound concentration was injected. For L2H2-6OTD, the dissociation constants was determined by fitting the binding curve using BIAevaluation software (GE Healthcare).

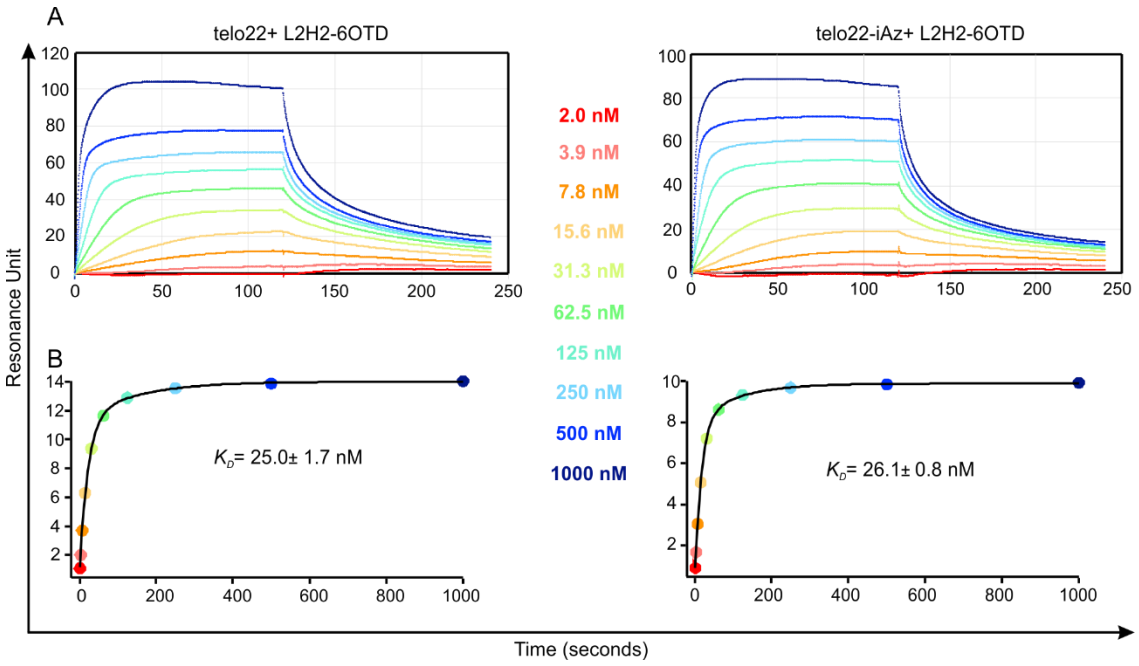

Figure S10. *Binding assays of the telomeric G-quadruplex sequences without (telo22) and with azide modification (telo22-iAz, 5'-Biotin-AGGGTTAGGGTTAGGGT/AzideT/AGGG) in presence of L2H2-6OTD monomer (0-1000 nM) by SPR (Surface Plasmon Resonance) in a HEPES Buffer [10 mM HEPES (pH 7.4), 3 mM EDTA and 0.005% surfactant P20 with 150 mM NaCl]. (A) Sensorgrams of the telo22 and telo22-iAz with the L2H2-6OTD at different concentrations. (B) Binding curves of the telo22 and telo22-iAz with the L2H2-6OTD.* K_D *depicts dissociation constant.*

15. Supporting Reference.

(S1) Ghimire, C.; Park, S.; Iida, K.; Yangyuoru, P.; Otomo, H.; Yu, Z.; Nagasawa, K.; Sugiyama, H.; Mao, H. *J. Am. Chem. Soc.* **2014**, *136*, 15537-15544.

(S2) Iida, K.; Tsubouchi, G.; Nakamura, T.; Majima, S.; Seimiya, H.; Nagasawa, K. *MedChemComm* **2013**, *4*, 260-264.

(S3) Iida, K.; Majima, S.; Nakamura, T.; Seimiya, H.; Nagasawa, K. *Molecules* **2013**, *18*, 4328-4341.

(S4) Krishna, H.; Caruthers, M. H. *J. Am. Chem. Soc.* **2012**, *134*, 11618-11631.

(S5) Yu, Z.; Koirala, D.; Cui, Y.; Easterling, L. F.; Zhao, Y.; Mao, H. *J. Am. Chem. Soc.* **2012**, *134*, 12338-12341.

(S6) Mao, H.; Luchette, P. *Sens. Actuators, B* **2008**, *129*, 764-771.

(S7) Léger, J. F.; Romano, G.; Sarkar, A.; Robert, J.; Bourdieu, L.; Chatenay, D.; Marko, J. F. *Phys. Rev. Lett.* **1999**, *83*, 1066-1069.

(S8) Yu, Z.; Mao, H. *Chem. Rec.* **2013**, *13*, 102-116.

(S9) Dhakal, S.; Cui, Y.; Koirala, D.; Ghimire, C.; Kushwaha, S.; Yu, Z.; Yangyuoru, P. M.; Mao, H. *Nucleic Acids Res.* **2013**, *41*, 3915-3923.

(S10) Dudko, O. K.; Hummer, G.; Szabo, A. *Proc. Natl. Acad. Sci. U. S. A.* **2008**, *105*, 15755–15760.

(S11) Dai, J.; Punchihewa, C.; Ambrus, A.; Chen, D.; Jones, R. A.; Yang, D. *Nucleic Acids Res.* **2007**, *35*, 2440-2450.

(S12) Dai, J.; Carver, M.; Punchihewa, C.; Jones, R. A.; Yang, D. *Nucleic Acids Res.* **2007**, *35*, 4927-4940.

(S13) Parkinson, G. N.; Lee, M. P.; Neidle, S. *Nature* **2002**, *417*, 876-880.

(S14) Wang, Y.; Patel, D. J. *Structure* **1993**, *1*, 263-282.

(S15) Phan, A. T.; Kuryavyi, V.; Luu, K. N.; Patel, D. J. *Nucleic Acids Res* **2007**, *35*, 6517-6525.

(S16) Lim, K. W.; Amrane, S.; Bouaziz, S.; Xu, W.; Mu, Y.; Patel, D. J.; Luu, K. N.; Phan, A. T. *J. Am. Chem. Soc.* **2009**, *131*, 4301-4309.

(S17) Hänsel, R.; Löhr, F.; Trantirek, L.; Dötsch, V. *Journal of the American Chemical Society* **2013**, *135*, 2816-2824.